Journal of Applied Physics ARTICLE scitation.org/journal/jap

Experimental and numerical study of a split cathode fed relativistic magnetron

Cite as: J. Appl. Phys. **130**, 034501 (2021); doi: 10.1063/5.0055118
Submitted: 26 April 2021 · Accepted: 28 June 2021 ·
Published Online: 15 July 2021

J. G. Leopold,[1,a)] M. Siman Tov,[1] S. Pavlov,[1] V. Goloborodko,[1] Ya. E. Krasik,[1] A. Kuskov,[2] D. Andreev,[2] and E. Schamiloglu[2]

AFFILIATIONS

[1]Department of Physics, Technion, Israel Institute of Technology, Haifa 3200003, Israel
[2]Department of Electrical and Computer Engineering, University of New Mexico, Albuquerque, New Mexico 87131-0001, USA

[a)]**Author to whom correspondence should be addressed:** leopoldjg@physics.technion.ac.il

ABSTRACT

The relativistic magnetron is one of the most efficient high power microwave (HPM) sources but pulse shortening, the result of explosive cathode plasma's radial expansion toward the anode, makes it impractical because the HPM pulse terminates much earlier than the applied voltage. We present experimental results of the operation of a relativistic magnetron fed by a split cathode. A split cathode [Leopold *et al.*, Phys. Plasmas **27**, 103102 (2020)] consists of a cathode placed upstream and outside the anode, connected by an axial rod to a reflector (a transverse conducting circular plate) placed downstream from the anode. The electron charge, emitted by an annular explosive cathode emitter, accumulates in the space between the cathode and the reflector and at the same time, screens the rod from explosive plasma formation. This accumulated space charge serves as the electron source for the magnetron. The explosive plasma developing on the emitter remains outside the magnetron and does not propagate into the anode while it operates. We compare the performance of the magnetron operating with a standard explosive emitting solid carbon cathode to that with a split cathode. The experiments demonstrate that whereas for the solid cathode, the microwave pulse developing in the magnetron suffers from pulse shortening, with a split cathode, the pulse survives as long as the amplitude of the applied voltage is sufficient for the magnetron's operation. We support the experiment by particle-in-cell simulations.

I. INTRODUCTION

Since the 1970s when the idea of relativistic magnetrons producing high power microwaves (HPMs) first materialized,[1] significant improvements were introduced in the operation of this device,[2] bringing it to a level considered at present as one of the most promising HPM sources. The ideas advancing the original work appear in a huge volume of literature and the timeline of these ideas has been recently reviewed.[3] We mention in this Introduction only work which seems most relevant to the present article.

One of the problems with relativistic magnetrons, common to other HPM devices, is pulse shortening due to the explosive cathode plasma's expansion toward the anode.[4] This not only shortens the duration of the microwave radiation and can cause mode competition but also interferes with the pulse repetition rate because the plasma needs to be cleared before the device can operate again. The introduction of the transparent cathode[5] reduced the plasma emission surface and drastically increased the efficiency of magnetron operation due to the better coupling experienced by electrons while drifting in the $E_r \times B_z$ fields with the azimuthal electric field E_θ of the electromagnetic wave. To further reduce the cathode plasma, the concept of the virtual cathode was introduced.[6] When a magnetized high-current electron beam, annular in particular, with sufficiently large current propagates in a conducting tube with increasing radial sections, a virtual cathode forms at the radius transition points from where currents flow in both directions. For two such transition points, the electron charge accumulates between the two virtual cathodes which can be used as the electrons source for a magnetron without the presence of a solid cathode. When a very strong axial magnetic field is applied, the accumulated charge increases while the energy of the electrons decreases due to the electric field of the accumulated space charge. This state of low energy, large accumulated electron charge is known as a *squeezed state*.[7] The disadvantage of the idea introduced[6] is that the downstream electron flow reaches the

magnetron's outer walls where the axial magnetic field stops to insulate the beam. To avoid this problem, another method was suggested to squeeze the beam between virtual cathodes, by shaping the axial magnetic field as a magnetic trap.[8] This method is very elegant but its disadvantage is that one needs to increase the magnetic field near the downstream virtual cathode, which makes the design of the magnetic field source difficult to realize. Furthermore, this idea requires an additional power supply to energize the mirror coil.

Recently, we introduced and experimentally tested a novel cathode, the split cathode,[9] which consists of a cathode holding an annular electron source, an axial rod placed at the center of the cathode holder, and a reflector connected to its downstream end. The split cathode forms a trap for the emitted electrons that fill the space between the cathode and the reflector having almost the same potential as the cathode potential without any axial current loss. This idea is more practical than the earlier virtual cathode methods. It was shown[9] that for the insulating axial magnetic fields needed in magnetrons, the accumulated charge is only partially squeezed. Confining the beam between two endcaps is not a new idea. It was first mentioned as a method to "suppress the shunt current"[10] but was not utilized since the electrostatic shields external to the magnetron interaction space would most likely suffer from explosive electron emission. Indeed, this is a possible problem, but if the tube outside the magnetron region has a large radius and the edges of the reflector are sufficiently smoothed, this breakdown can be avoided. The authors introduced an inverted magnetron[10] for which they state that endcaps do not break down. This is because the central anode is kept at the high voltage (HV) and the cathode is grounded. Such an inverted magnetron was recently developed with an elegant axial output design.[11] The design of the split cathode can be adjusted to solve the problem of pulse shortening in an inverted magnetron as well and can be applied for both radial[12] or axial[13] extraction techniques.

In this article, we present experimental data for a relativistic magnetron operating with a split cathode. These results are compared with results obtained in experiments with the same magnetron operating with a common explosive emission cathode.

The remainder of this article is organized as follows. Section II describes the experimental setup and diagnostics employed. Section III presents the experimental results and Sec. IV presents a comparison between the experimental and simulation results. Finally, Sec. V summarizes the conclusions.

II. EXPERIMENTAL SETUP AND DIAGNOSTICS

In these experiments, we used the same setup as that used in our earlier research[9] but we replaced the anode with a relativistic A6 magnetron. The external and internal radii of the magnetron anode resonator cavity were 43 and 21 mm, respectively, and we tested a 60 mm long anode block. The magnetron anode block was inserted coaxially inside a 124 mm diameter, 350 mm long

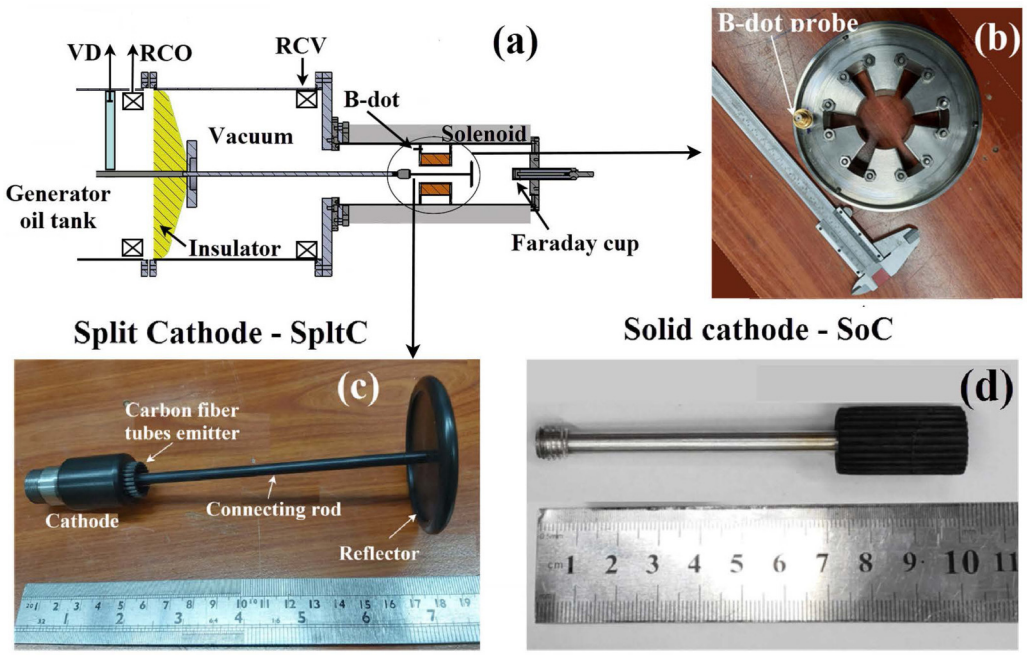

FIG. 1. (a) The experimental setup of the magnetron set to operate with a split cathode. The locations of the various probes, VD, RCO, RCV, and B-dot, explained in the text, are pointed out by arrows. The magnetron and the split cathode are encircled and detailed in (b) where the connector to one of the B-dot probes inside the space above the magnetron is pointed out on the A6 magnetron used in the experiment. (c) A picture of the split cathode, SpltC, and its parts and (d) the solid carbon cathode, SoC. The reflector can be attached to the SoC's free end by the connecting rod, which makes it a solid cathode with a reflector (SoCR) arrangement.

stainless-steel tube. All cavities were open through $58 \times 10\ mm^2$ rectangular slots to a circular cavity between the magnetron's outer radius and the tube's internal radius [see Fig. 1(a)].

An external solenoid was used to magnetically insulate the electron beam. The solenoid, wound around the experimental tube [see Fig. 1(a)], provided a uniform axial magnetic field. The solenoid is energized by a current pulse with a half-period of 15 ms produced by the discharge of a 4 mF capacitor charged to a voltage ranging from 180–600 V, corresponding to a magnetic field ranging from 0.16 to 0.48 T. The pulsed power source used to power the magnetron in experiments was a Marx generator. Once charged to a voltage of ±33 kV, a negative polarity high voltage (HV) of ∼250 ns long pulse of an amplitude of ∼180 kV with a matched resistive load of ∼80 Ω is produced. The vacuum in the experimental system was kept at a level of 10^{-3} Pa by a turbo-molecular pump.

In the experiments, we compare the magnetron's performance when fed by either a split cathode (SpltC) [Fig. 1(c)] or solid graphite cathode [Fig. 1(d)] with (SoCR) and without a reflector (SoC). The exact location of each of these cathode arrangements feeding the magnetron is seen in Fig. 4. The split cathode had the same design as that described earlier,[9] namely, it comprises of 20 carbon capillary tube emitters (5 mm long and 1.5 mm/0.75 mm in outer/inner diameter each) inserted into holes along a 16 mm diameter circular perimeter of a hollow aluminum cathode. At the top edge of each of these carbon capillary tubes, where the electric field enhancement is highest, explosive emission plasma spots appear. Thermal expansion makes the individual plasma plumes to overlap to a plasma ring emitting an annular electron beam. This plasma does not propagate fast enough to reach the interaction region of the magnetron and causes pulse shortening during the high voltage pulse. The non-emitting cathode holding the emitters [see Fig. 1(c)] had an outer diameter of 25 mm to prevent the upstream flow of electrons. The axial distance between the capillaries and the anode was 20 mm. The reflector was a 2 mm thick, 40 mm diameter aluminum disk with a 6 mm diameter ring at its periphery to reduce the edge electric field. The reflector was connected to the cathode center using a 5 mm diameter aluminum central rod. For the SoCR, we attached the reflector to the downstream end of the SoC. The cathode, reflector, and rod were coated by an 80 μm-thick Al_2O_3 ceramic layer to protect these parts from electron emission. We should point out that, following the experiments, no damage to this coating was seen along the rod, which is an indirect proof that no explosive emission occurs on its surface. The distance of the reflector from the downstream end of the anode was 40 mm. The solid graphite cathode had the same diameter, 16 mm, as the diameter of carbon capillaries, and its length was equal to half the anode length. The most important difference between the split cathode and the solid cathodes is that the emitter of the SpltC is placed upstream in the larger radius tube and outside the magnetron interaction space at a sufficient distance so that the plasma remains outside the magnetron.

The voltage pulses were measured using a resistive voltage divider (VD) placed inside the transformer oil-filled tank at the output of the Marx generator. The total current, $I_t = I_m + I_r + I_{FC}$, was measured using a self-integrating Rogowski coil placed at the same position as the VD in the Marx generator's oil tank (RCO). Here, I_m is the magnetron current, I_r is the return current, which is the current of the electrons flowing upstream from the cathode, and I_{FC} is the current flowing downstream from the magnetron in the absence of the reflector measured by a low-inductance Faraday Cup (FC) placed 80 mm downstream from the magnetron. An additional Rogowski coil is placed inside the vacuum chamber following the generator (RCV). The magnetic field lines decrease upstream from the position of RCV; therefore, the current measured by the RCV is $I_v = I_t - I_r$, and I_r ends up on the walls of the large vacuum chamber upstream from the RCV. When the reflector is used, $I_{FC} = 0$, and $I_m = I_v$ and $I_r = I_t - I_v$. The positions of these diagnostic probes are pointed out in Fig. 1(a).

The system at this point was not designed to radiate; rather, we measured the generated microwaves using two B-dot probes assembled in stainless-steel cups placed in the space between the tube and anode at the center of two adjacent anode slots. The location of one of these is seen in Fig. 1(b). These probes were calibrated using a B-dot probe connected to a Rohde & Schwarz ZVL6 (9 kHz–6 GHz) network analyzer placed inside one of the magnetron's cavities. Microwaves in the frequency range of 1–6 GHz were radiated into this cavity and measured by the B-dot located in the cup outside the anode. Using the measured input, the reflected and transmitted powers, the coupling coefficient of the B-dot as a function of the microwave frequency was obtained. The waveforms of the current, voltage, and microwaves were acquired using an Agilent Infinium DSO81204B (12 GHz, 40 Gs/s) oscilloscope.

III. EXPERIMENTAL RESULTS

Waveforms of the voltage, V, the total current I_t, the current I_v, and the microwave signal measured by one of the B-dot probes are shown in Fig. 2 for a 60 mm long magnetron for a magnetic field of 0.2 T. Three cathode arrangements are compared: a solid graphite cathode (SoC), the same but with a downstream reflector (SoCR), and last, a split cathode (SpltC). The signals measured by the B-dot probe can be compared relative to the values measured for the case of the SoC normalized to the maximum observed value.

One can see that, for both solid cathode cases, the waveforms of the voltage V, and currents I_t and I_r are very similar. During the first ∼30 ns, the voltages rise to ∼90−110 kV and the total currents are ∼1.6−1.7 kA for the SoCR and SoC cases, respectively. These values stay nearly constant for an additional ∼30 ns. Then, up to ∼130−150 ns, the voltage for both cases increases, reaching ∼130 kV, while the total current increases to ∼3 kA. Without the reflector, SoC, the magnetron current reaches a maximum of ∼1.4 kA at ∼100 ns, stays nearly constant for ∼100 ns, and then decreases following the voltage pulse. With the reflector, SoCR, the magnetron current keeps increasing even after the voltage peaks. The axial current collected by the FC, I_{FC}, present only in the absence of the reflector [Fig. 2(a) for the SoC case] increases and then stays almost constant as the voltage decreases.[16] This increase is probably due to the partial compensation of the electron space charge by ions emitted from the plasma formed on the FC surface. With the split cathode, SpltC, the voltage rises to ∼220 kV during ∼30 ns, much higher than the value reached for the solid cathode cases. It remains constant for ∼50 ns and then decreases gradually.

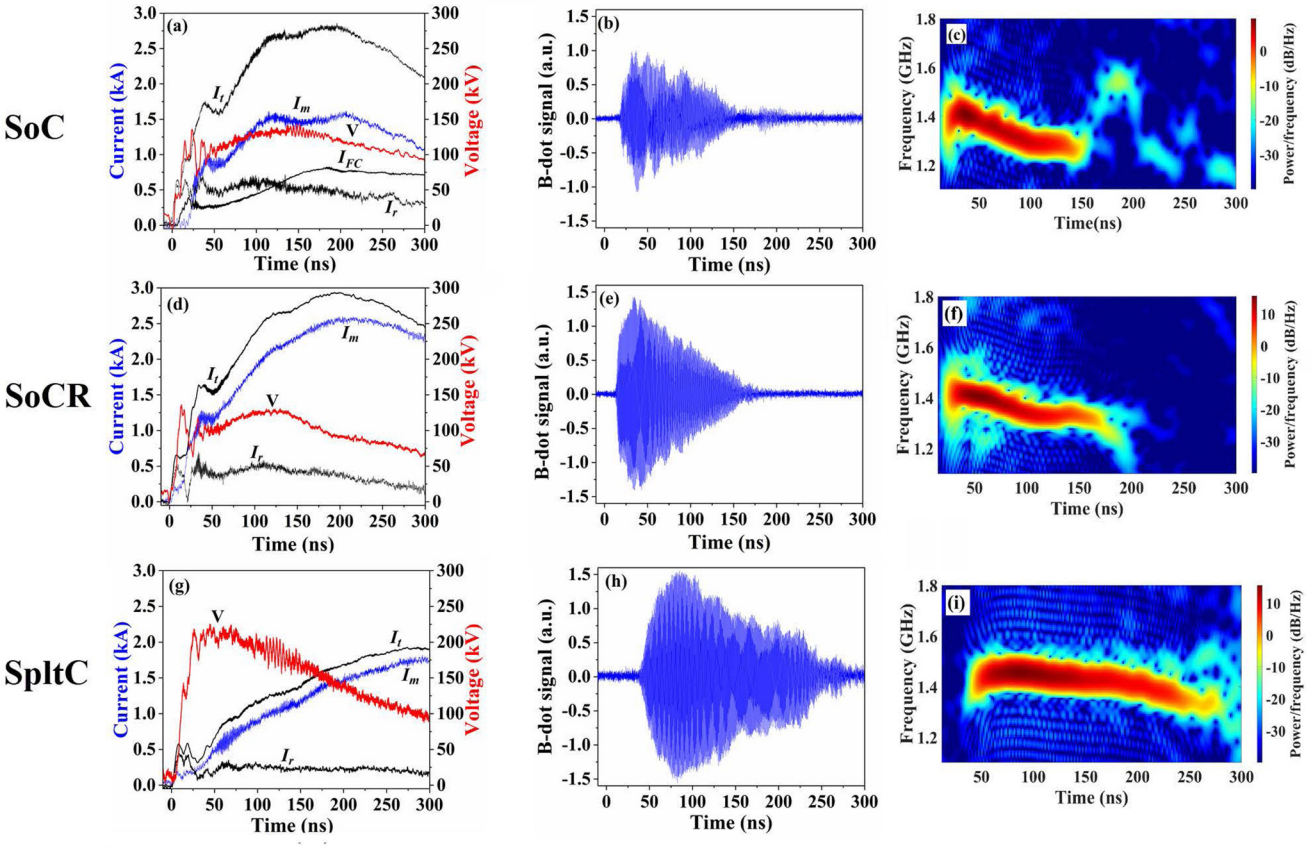

FIG. 2. Experimental results for the SoC case (solid cathode no reflector) [(a)–(c)], the SoCR case (solid cathode + reflector) [(d)–(f)], and the SpltC (split cathode) [(g), (e), and (h)]. In (a), (d), and (g), the measured voltage, V, the currents, I_t, and I_v, and the evaluated currents, I_v and I_n are displayed. The measured value of I_{FC} appears only for the SoC case. (b), (e), and (h) display the signal measured by one of the B-dot probes whereas (c), (f), and (i) show the time–frequency plots derived from the signals measured by the B-dot probe.

At the same time, the total and the magnetron currents increase, while the difference between the two, I_r, keeps nearly constant.

The B-dot signal, that is, the microwave field, starts when the magnetron current reaches ∼0.6 kA for the cases of SoC and SoCR and ∼0.4 kA for the SpltC case. The earliest start is for the SoCR case (∼15 ns), then for the SoC (∼25 ns), and finally for the SpltC case (∼40 ns). For the latter, the charge accumulated between the cathode and the reflector does not spread toward the magnetron unless it is sufficiently high.[9] Note, also, that I_r is much smaller for this case. For the solid cathode cases, the microwave signal is higher when the reflector is present. However, for both these cases, there is a fast decrease in the signal amplitude and the pulse duration does not exceed ∼120 ns. The frequency of the microwave fields for both solid cathode cases was 1.4 GHz, which reduces at ∼100 ns to 1.3 GHz, suggesting mode competition. In contrast to this behavior obtained for the solid cathode cases, with the SpltC, the duration of the microwave generation lasts for ∼210 ns and the frequency is 1.44 GHz and remains almost unchanged for ∼200 ns.

In Fig. 3, the experimental input electrical power and the average output microwave power as a function of time are plotted for all three cathode arrangements.

The output microwave power is calculated averaging the signals obtained by the calibrated B-dot probe in Figs. 2(b), 2(e), and 2(h). The maxima of the average output microwave power in Fig. 3(b) are ∼15, ∼38, and ∼45 MW for the SoC, SoCR, and the SpltC cases, respectively. Note that for the solid cathode cases, there is a plateau in the interval ∼30–60 ns in the input electrical power at ∼160 MW [see insert in Fig. 3(a)] followed by an increase to above 300 MW. This increase is probably the result of the cathode plasma's radial expansion toward the radius (for our experimental conditions at $r \sim 13$ mm) where magnetic insulation of the electrons is violated [see Figs. 2(a) and 2(d)]. This process does not cause a short circuit; in fact, the input power for the SoC remains constant at ∼350 MW for almost ∼50 ns, the result of the increasing axial FC current that drains electrons from the anode gap and adds azimuthal self-magnetic field. For the SoCR, the reflector returns these electrons into this gap, decreasing the self-magnetic field, which results in a

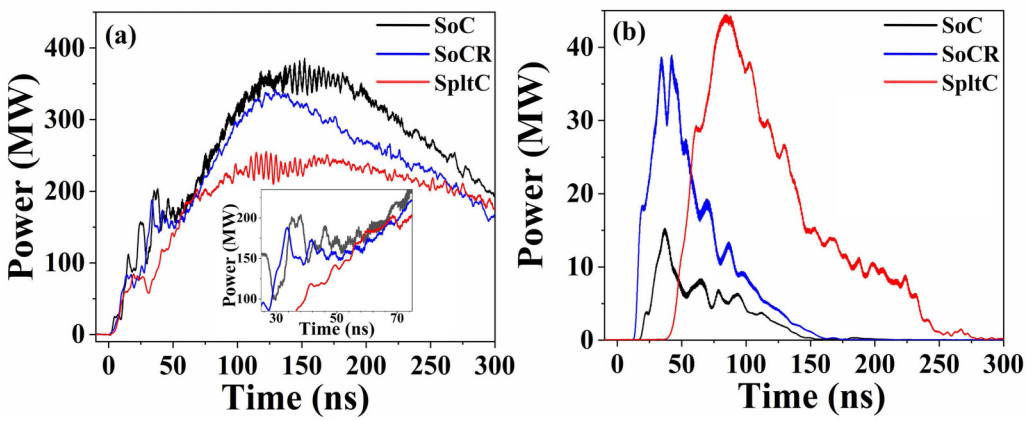

FIG. 3. (a) The experimental input power calculated from the total experimental electrical power $I_t \times V$ (Fig. 2) and (b) the average output microwave power vs time for all three cathode arrangements. The inset in (a) is an enlarged view of the time interval 25–75 ns.

larger current to the anode and an earlier decrease in the input power. The output microwave power for the SoC and SoCR peak in the time interval which can be seen in the inset in Fig. 3(a) followed by pulse shortening due to the plasma effects. The SpltC behaves in a different way. The input power rises in ∼100 ns (remember, the rise time of the voltage is ∼30 ns) and then it keeps almost constant for ∼200–250 ns when it starts to slowly decrease. For the SpltC with the emitter outside the magnetron, there should be no plasma in the space enclosed by the anode. After ∼50 ns, sufficient electron charge has accumulated inside this space and drifted toward the anode to start radiating microwave power [see Fig. 3(b)]. The output microwave power peaks when the input power is at the plateau and keeps on for a much longer period than for the solid cathode cases. In Fig. 2(g) for the SpltC, the voltage starts to decrease at ∼75 ns but the currents keep increasing. At present, we do not know what are the phenomena governing this process. Nevertheless, one can consider two reasons: (a) the plasma, generated on the tips of the carbon fibers placed 2 cm upstream from the anode, expands preferably in the axial direction (the axial velocity can be estimated to be $>10^7$ cm/s and $\sim 10^6$ cm/s in the radial direction),[15] reducing the emitter–anode distance by a few mm during ∼200 ns resulting in increasing current and (b) expansion of the electron cloud inside the anode due to repulsive Coulomb forces.

Following this discussion, to estimate the average magnetron efficiency for the different cathode arrangements, it is reasonable to divide the maxima of the output microwave power by the values of the corresponding input electrical power at the times when the average microwave power is maximal, resulting in ∼9%, ∼21%, and ∼21%, for the SoC, SoCR, and the SpltC cases, respectively. The lower efficiency for the microwave generation for the SoC case is the result of the "power loss" to the FC current.

IV. SIMULATION RESULTS AND COMPARISON TO EXPERIMENT

The three situations studied experimentally in Sec. III were simulated using the MAGIC PIC code.[14] The geometry of these cases is displayed in Fig. 4. The simulated magnetron length was 6 cm and all other dimensions are the same as those in the experiments. A uniform axial magnetic field of 0.2 T is applied in all cases. We do not simulate the large upstream vacuum container, the generator, and its oil tank [see Fig. 1(a)]. The system in Fig. 4 as in Fig. 1 is not designed to radiate microwave power radially or axially through open boundaries.

The experimental results in Sec. III demonstrate that for the two solid cathode cases [Figs. 4(a) and 4(b)], the cathode plasma starts to expand at ∼60 ns with pulse shortening setting in almost at the same time. The simulations do not consider the formation and expansion of explosive plasma on the surface of the solid cathode or the tip of the annular emitter. Thus, PIC simulations of the SoC and SoCR are relevant only up to ∼60 ns, the end of the "plateau" in the inset in Fig. 3(a). No pulse shortening develops with the split cathode up to at least ∼150–200 ns [see Fig. 3(b)].

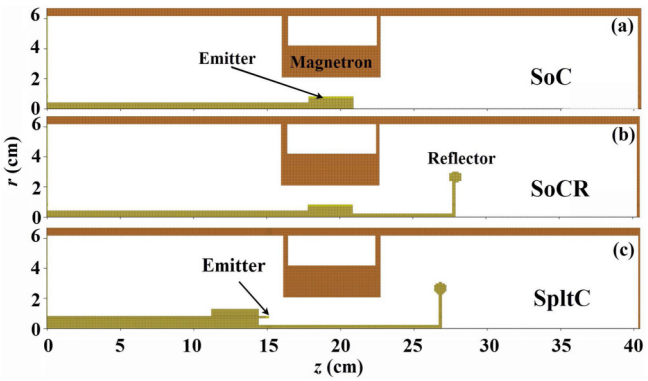

FIG. 4. [r,z] cross section of the three PIC simulated cases studied. (a) A solid cathode placed at the axial magnetron center. (b) A reflector connected by a central rod is added. (c) A split cathode having an emitter outside the interaction region.

For these reasons, even though we do not simulate the dynamics of the plasma, it is worthwhile to compare the behavior of these cathodes in particular since the split cathode suggested in Ref. 9 has not been tested in a magnetron before.

For all cases, a voltage of 220 kV rising in 30 ns and kept constant up to 150 ns is applied to the upstream open boundary seen in Fig. 4, but as the voltage increases and the current starts to be emitted and then flows to the anode, the impedance (~123 Ω) of the upstream system affects the voltage. For a SoC magnetron [Fig. 4(a)], in addition to the radial current from the emitter to the anode block, axial currents develop flowing in both upstream (I_r) and downstream directions (I_{FC}). Figures 5(a)–5(c) display the time

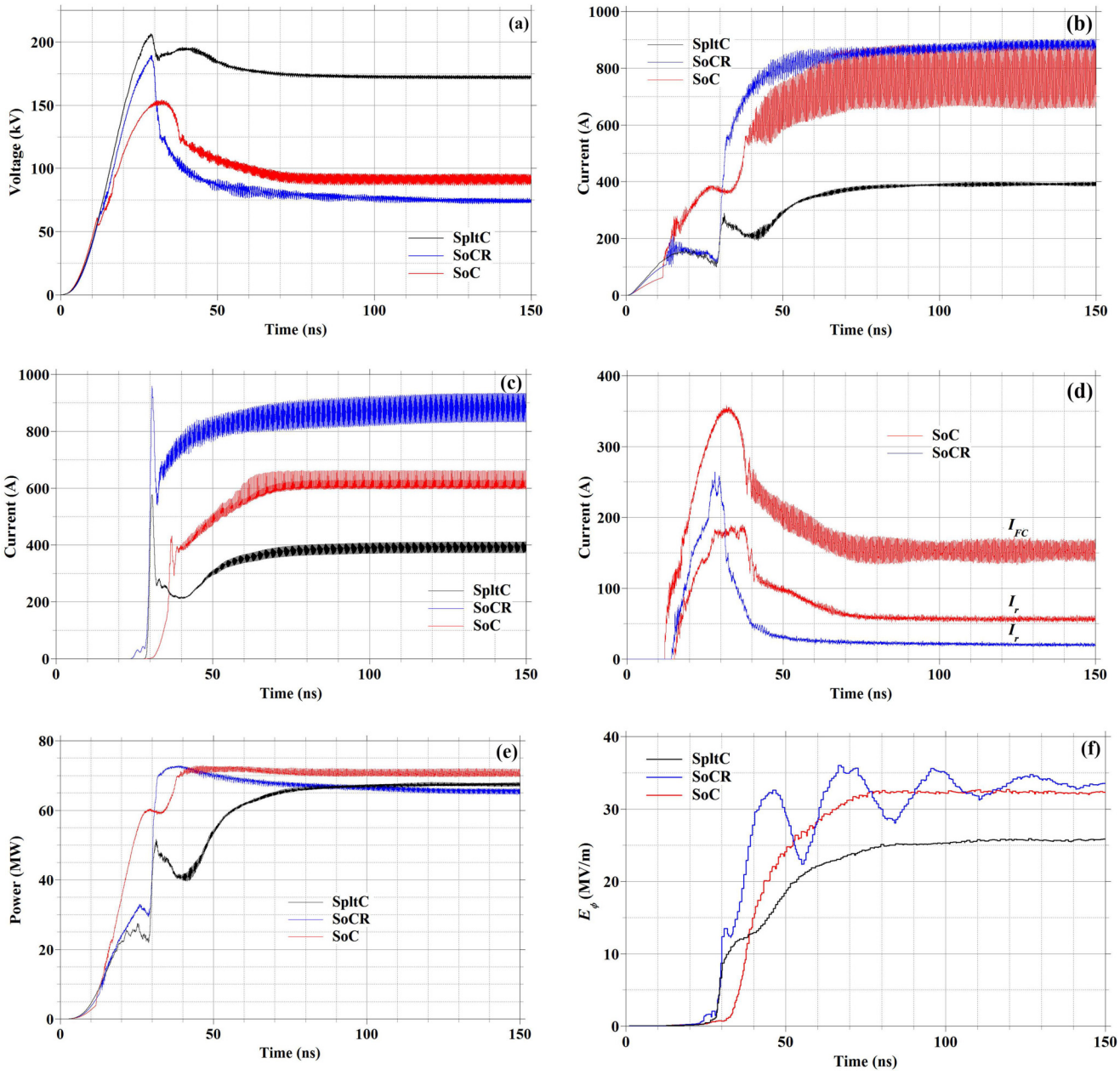

FIG. 5. The results of the PIC simulations vs time for the three cases in Fig. 3. (a) The applied voltage, (b) the total current, (c) the magnetron current, (d) the axial currents, (e) the input power, and (f) the envelope of the absolute value of the azimuthal electric field at the center of one of the magnetron cavities.

dependence of the voltage, the magnetron current, and the total current, respectively, for the three cases. The voltage for all cases increases during the rise time and then adjusts as the simulated system reaches a steady matched impedance state. Note that the steady state voltage for the SoC case is slightly higher than that for the SoCR case and both are almost half that obtained for the SpltC case. The simulated values of the voltages and magnetron currents are close to the experimental values over the time period ∼30 −60 ns. Following this time period, for both SoC and SoCR cases, the experimental voltage increases slightly but the magnetron current increases considerably. This current increase is not seen in the simulations because the plasma is not present and, therefore, for the solid cathode cases, the simulations can be compared to the corresponding experiments in Fig. 2 only up to ∼60 ns. The difference between the SoC and the SoCR is that for the latter, no axial current flows downstream from the reflector, and the upstream axial current is smaller than that in the absence of the reflector [Fig. 5(d)]. The experimental values behave in a similar way up to ∼60 ns.

Note that, when more current flows axially [Fig. 5(d)], less current flows to the magnetron [Fig. 5(c)].[16] In the experiment, the upstream axial current reaches the walls of the vacuum chamber, which is outside the simulated volume. The voltage decreases once currents reach the magnetron or the walls. For the simulated SpltC case, no axial currents form, and the space between the reflector and the cathode body contains the entire electron charge.[9] For the SpltC, the magnetron current is low but the voltage is high. For the two solid cathode cases, the voltage is nearly half of this value. Nevertheless, the input power for all three cases is almost the same.

The azimuthal electric field component of the microwave field developing in one of the magnetron cavities for all three cases is shown in Fig. 5(f). The maximum value of this field for all cases is of the same order of magnitude, slightly lower for the SpltC case, suggesting that the efficiencies are also similar. This agrees with the estimated experimental efficiencies presented in Sec. III for the SoCR and SpltC cases, which are almost equal but differ from the results obtained for SoC. The frequencies of the signals in Fig. 5(f) are 1.55, 1.50, and 1.52 GHz for the SoC, SoCR, and SpltC cases, respectively. Considering the differences between the experimental and simulated systems, these are sufficiently close to the experimental frequencies. On the other hand, the frequencies for the three cases are within a few percent, as in the experiment. The simulations, apart from neglecting the plasma formation, do not consider the entire geometry of the system and the emitting surfaces are not modeled exactly as in the experiment. All these factors are probably responsible for the differences.

V. SUMMARY

The results of the experiments presented in this article confirm that a split cathode, as an electron source in relativistic magnetrons, can successfully replace explosive emission solid cathodes. It was shown that the microwave power and the efficiency of microwave generation with the split cathode are comparable to those obtained with a solid cathode. Moreover, as expected,[9] the duration of the microwave pulse is considerably longer with a split cathode than when common cathodes feed the same magnetron. With solid cathodes, pulse shortening is observed. Numerical simulations support the experimental results.

ACKNOWLEDGMENTS

At the Technion, this work was supported by Technion (Grant No. 2029541) and ONRG (Grant No. N62909-21-1-2006) and at the University of New Mexico by AFOSR (Grant No. FA9550-19-1-0225) and ONR (Grant No. N00014-19-1-2155). The Technion group could not have performed the experiments without the assistance of S. Gleizer and E. Flyat.

DATA AVAILABILITY

The data that support the findings of this study are available from the corresponding author upon reasonable request.

REFERENCES

[1]G. Bekefi and T. J. Orzechowski, Phys. Rev. Lett. **37**, 379 (1976).
[2]J. Benford, J. A. Swegle, and E. Schamiloglu, *High Power Microwaves*, 3rd ed. (CRC Press, Boca Raton, FL, 2015).
[3]D. Andreev, A. Kuskov, and E. Schamiloglu, Matter Radiat. Extremes **4**, 067201 (2019).
[4]D. Price, J. S. Levine, and J. N. Benford, IEEE Trans. Plasma Sci. **26**, 348 (1998).
[5]M. Fuks and E. Schamiloglu, Phys. Rev. Lett. **95**, 205101 (2005).
[6]M. I. Fuks, S. Prasad, and E. Schamiloglu, IEEE Trans. Plasma Sci. **44**, 1298 (2016).
[7]A. M. Ignatov and V. P. Tarakanov, Phys. Plasmas **1**, 741 (1994).
[8]M. Fuks and E. Schamiloglu, Phys. Rev. Lett. **122**, 224801 (2019).
[9]J. G. Leopold, Y. E. Krasik, Y. P. Bliokh, and E. Schamiloglu, Phys. Plasmas **27**, 103102 (2020).
[10]R. A. Close, A. Palevsky, and G. Bekefi, J. Appl. Phys. **54**, 4147 (1983).
[11]T. P. Fleming, IEEE Trans. Plasma Sci. **48**, 3076 (2020).
[12]Y. Hadas, A. Sayapin, Y. E. Krasik, V. Bernshtam, and I. Schnitzer, J. Appl. Phys. **104**, 064125 (2008).
[13]M. I. Fuks and E. Schamiloglu, Proc. SPIE **4720**, 18 (2002).
[14]B. Goplen, L. Ludeking, D. Smith, and D. Warren, Comput. Phys. Commun. **87**, 54 (1995).
[15]S. P. Bugaev, V. I. Kanavez, V. I. Koshelev, and V. A. Cherepanov, *Relativistic Multi Wave Microwave Generators* (Siberian Division, Novosibirsk, 1991), pp. 81–94 (in Russian).
[16]J. G. Leopold, A. S. Shlapakovski, A. Sayapin, and Y. E. Krasik, IEEE Trans. Plasma Sci. **43**, 3168 (2015).